Applied Catalysis B: Environmental 162 (2015) 133–140

Contents lists available at ScienceDirect

Applied Catalysis B: Environmental

journal homepage: www.elsevier.com/locate/apcatb

The durability of carbon supported Pt nanowire as novel cathode catalyst for a 1.5 kW PEMFC stack

Bing Li[a,b,*], Drew C. Higgins[c], Qiangfeng Xiao[d], Daijun Yang[a,b], Cunman Zhng[a,b], Mei Cai[d], Zhongwei Chen[c], Jianxin Ma[a,b]

[a] School of Automotive Studies, 4800 Caoan Road, Tongji University (Jiading Campus), Shanghai 201804, China
[b] Clean Energy Automotive Engineering Center, Tongji University, Shanghai 201804, China
[c] Department of Chemical Engineering, University of Waterloo, Waterloo, ON, Canada N2L 3G1
[d] Research & Development Center, General Motors, Warren, MI 48090, United States

ARTICLE INFO

Article history:
Received 10 March 2014
Received in revised form 18 June 2014
Accepted 23 June 2014
Available online 30 June 2014

Keywords:
PtNW/C electrocatalyst
Durability
Dynamic drive cycle testing
Stack
PEMFCs

ABSTRACT

Carbon supported platinum nanowires (PtNW/C) synthesized by a simple and inexpensive template-free methodology has been used for the first time as a cathode catalyst in a 15 cell with an active area of 250 cm^2, 1.5 kW proton exchange membrane fuel cell (PEMFC) stack. Drive cycle testing along with in-situ and ex-situ accelerated degradation testing (ADT) showed that the PtNW/C catalyst exhibited better durability than commercial Pt/C. After a 420 h dynamic drive cycle durability testing, the PEMFC stacks exhibited a performance degradation rate of 14.4% and 17.9% for PtNW/C and commercial Pt/C based cathodes, respectively. It was found that the majority of performance loss was due to degradation of the commercial Pt/C anode materials, resulting from the rapidly changing load frequencies used in the testing protocol, ultimately leading to harsh fuel/air starvation conditions and subsequent Pt nanoparticle growth and agglomeration. Notably, based on post-testing characterization, the structure, electrochemically active surface area (ECSA) and oxygen reduction activity of the PtNW/C cathode catalyst remained unchanged during the drive cycling, indicating its excellent stability under these practical conditions. Conversely, when using commercial Pt/C as a cathode catalyst, significant Pt nanoparticle growth and agglomeration were observed, resulting in the reduced PEMFC stack durability. Therefore, PtNW/C materials are presented as promising replacements to conventional Pt/C as cathode electrocatalysts for PEMFCs, and particularly demonstrate improved stability under the practical conditions encountered for automotive applications.

1. Introduction

Proton exchange membrane fuel cells (PEMFCs) are considered promising sustainable energy technologies due to their high efficiency, quick startup, relatively low operating temperature, simple construction, good dynamic performance, and environmental benignity [1]. For these reasons, the major application potential has been focused on the transportation sector. At present, the major barrier preventing the successful commercialization of PEMFCs is its performance and insufficient durability [2]. State of the art carbon-supported platinum nanoparticles (Pt/C) are the most widely used catalysts due to their high catalytic activity toward the sluggish oxygen reduction reaction (ORR). However, reducing the overall expensive platinum loading at the cathode, along with improving the long-term operational durability of the cathode catalysts remain two key technical challenges that need to be addressed. Nanostructure control strategies have been effective in improving electrocatalyst stability, whereby extended surface Pt and Pt-alloy structures have been demonstrated to result in increased resistance to Pt rearrangement or dissolution [3–5]. Particularly, Pt-based nanowires (NWs) [6,7], nanowire networks (NWNs) [8] and nanoarrays (NA) [9] have recently been shown capable of significantly improving upon the ORR activity and/or durability of commercial Pt/C catalyst. Recently, Sun et al. [10–13] reported that Pt-based NWs synthesized by template-free methods can provide significantly improved specific and mass based activities, coupled with improved operational durability in

* Corresponding author at: Clean Energy Automotive Engineering Center, Tongji University, Shanghai 201804, China. Tel.: +86 21 6958 3891/+86 21 6958 3796; fax: +86 21 6958 3850.
E-mail addresses: libing210@tongji.edu.cn (B. Li), yangdaijun@tongji.edu.cn (D. Yang).

http://dx.doi.org/10.1016/j.apcatb.2014.06.040
0926-3373/

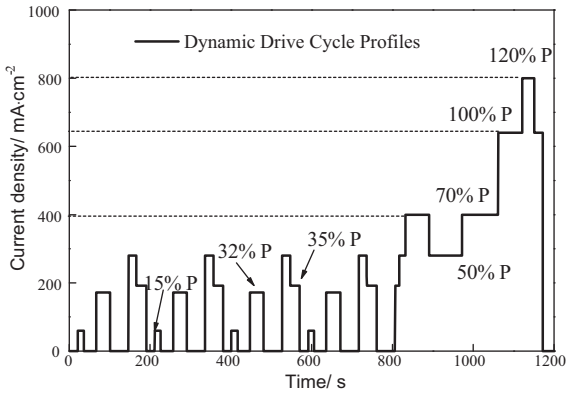

Fig. 1. Profile of dynamic load cycle used for durability testing.

comparison to commercial Pt/C. However, the aforementioned studies have relied on half-cell investigations in order to evaluate the ORR activity and stability. No reports currently exist reporting electrode and cell preparation, stack integration, along with performance and drive cycle durability testing of PtNW based catalysts. These evaluations are highly necessary in order to evaluate the practical application potential of this unique catalyst technology.

In the present work, we prepare carbon-supported platinum nanowires (PtNW/C) using this simplistic and inexpensive template-free methodology. In-situ and ex-situ accelerated degradation testing (ADT) was employed to evaluate the durability of these materials. Furthermore, as-prepared PtNW/C was used as a cathode catalyst for a 1.5 kW FC stack, and a 420 h durability testing based on simulated drive cycles was conducted in order to elucidate the practical performance and evaluate the feasibility of PtNW/C catalyst for automotive applications. Finally, several post-drive cycle characterization techniques were applied to analyze the mechanistic pathways of stack performance degradation, providing fundamental insight that will aid in the design of engineered cathode structures with improved durability.

Table 1
Parameter of JM Pt/C and PtNW/C catalysts.

Catalyst	Initial ECSA ($m^2\ g^{-1}$)	ECSA after 1500 cycles ($m^2\ g^{-1}$)	Maintenance rate (%)
JM Pt/C	50	38.35	76.7
PtNW/C	41	39.73	96.9

2. Experimental

2.1. Materials and catalyst synthesis

PtNW/C were prepared by modifying a procedure reported previously [10]. In a typical synthesis, a mixed aqueous solution of $H_2PtCl_6{\cdot}6H_2O$ and 98% pure HCOOH, as well as an appropriate amount of carbon black (Vulcan XC72) was placed in a 100 mL glass beaker at room temperature. To control the loading of Pt on the carbon support at 40 wt.% Pt, 0.15 g $H_2PtCl_6{\cdot}6H_2O$ and 30 mL HCOOH were dissolved in 50 mL ultrapure water. 75 mg of carbon black (Vulcan XC72) was the dispersed in the above solution by ultrasonication (Model B25, BRT) for 60 min. This solution was left stagnant and allowed to react for 72 h, after which the product was collected, washed and dried completely. The final catalyst

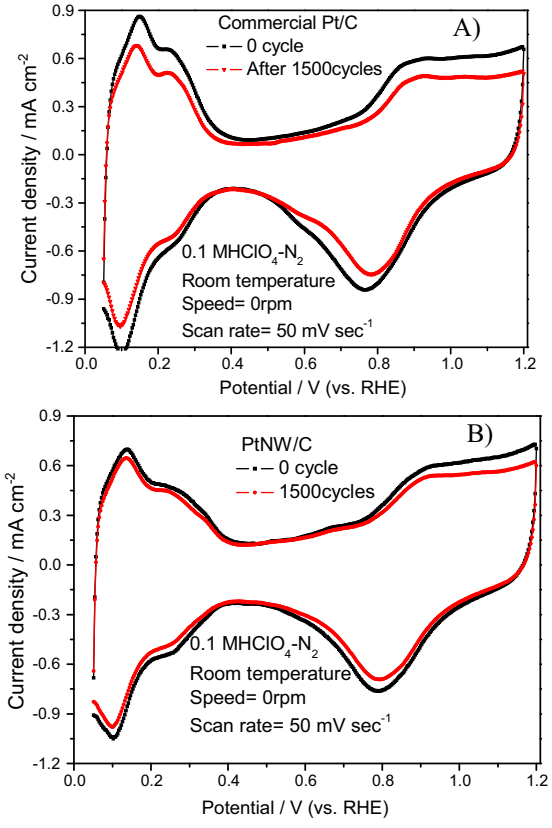

Fig. 2. CV curves of before and after 1500 cycles for (A) commercial Pt/C and (B) PtNW/C in 0.1 M $HClO_4$ at the ambient solution temperature in N_2, Scan rate: 50 mV s^{-1}, electrode area: 0.283 cm^2; catalyst loading: 28 μg cm^{-2}.

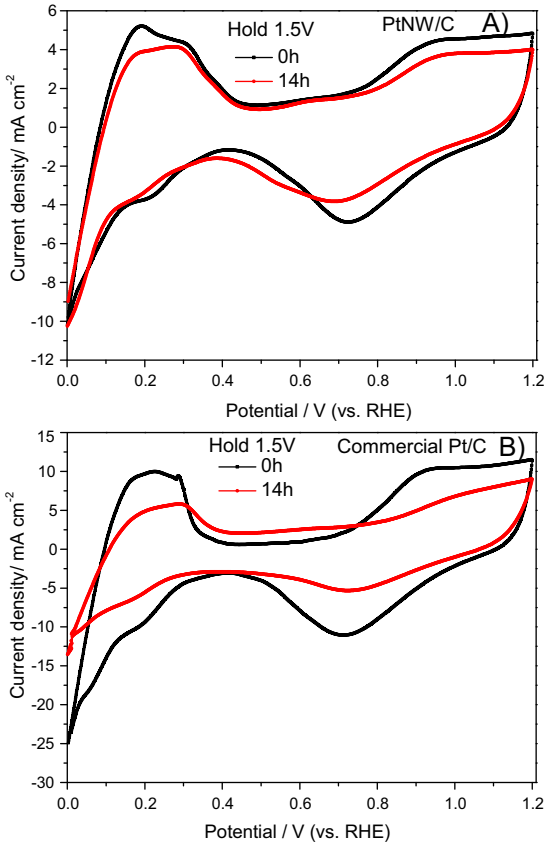

Fig. 3. CV curves of before and after 14 h ADT (hold 1.5 V) for MEA prepared with (A) PtNW/C and (B) commercial Pt/C, respectively. CE: 400 mL min^{-1} H_2, WE: 400 mL min^{-1} N_2.

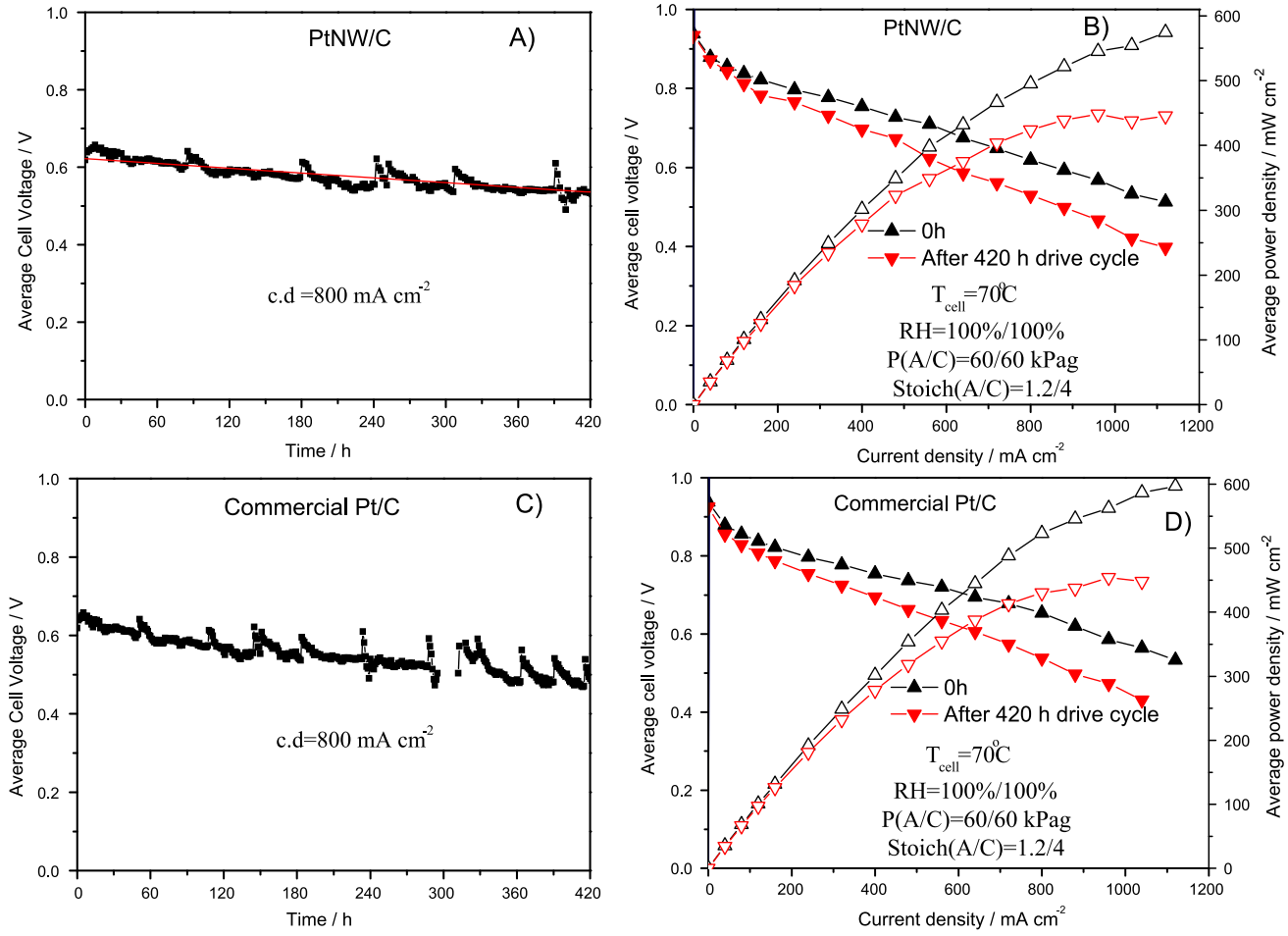

Fig. 4. Average cell power as a function of the operation time, (A) PtNW/C and (C) commercial Pt/C; (B) *I–V* and *I–P* curves of PtNW/C; (D) *I–V* and *I–P* curves of commercial Pt/C.

powders were obtained by a heat-treatment process carried out at 200 °C in a tube furnace under a N_2/H_2 (9:1) gas mixture. The duration of treatment was 2 h with the flow rate was 670 mL min^{-1}.

2.2. Characterization of catalyst

X-ray diffraction (XRD) patterns were collected using a PHILIPS PW 3040/60 powder diffractometer with a Cu *Kα* radiation (Å) source. A 40 kV accelerating voltage and 40 mA beam current at 25 °C was used. The data was collected between 2*θ* values of 20° to 100° at a scan rate of 1.20° min^{-1}. The collected patterns were then processed using JADE5 software. The morphology of the PtNW/C catalyst before and immediately following durability testing were observed using a transmission electron microscope (TEM) (model JEM 2010, JEO) operating at 200 kV.

2.3. Electrochemical testing

In order to evaluate catalyst activity, 4 mg of PtNW/C were suspended in 2 mL methanol/water/Nafion solvent to prepare a catalyst ink, which was ultrasonicated (Model B25, BRT) for 2 h to ensure good catalyst dispersion. Then, 10 μL of the ink was deposited onto a clean glass carbon working ring disk electrode (RDE) (Model AFMSRCE, 6 mm diameter, Pine) twice and allowed to dry under ambient conditions. PtNW/C catalysts were tested for their electrochemical ORR activity in a glass cell consisting of a three-electrode system in 0.1 M $HClO_4$ electrolyte at room temperature. The reversible hydrogen electrode (RHE) was used as the reference electrode, and Pt foil was used as the counter electrode. Cyclic voltammetry (CV) was carried out by six repeated cycles between 0.05 and 1.2 V vs RHE at a scan rate of 50 mV s^{-1}. Linear sweep voltammetry (LSV) was tested in a potential range of 0.05 to 1.20 V in the positive direction at a scan rate of 5 mV s^{-1} and rotation speed of 1600 rpm [14,15].

2.4. Fabrication of membrane electrode assemblies (MEAs)

MEAs with an active area of 250 cm^2 were prepared using either PtNW/C or commercial Pt/C based cathodes. These electrodes were prepared by first dispersing PtNW/C in 5 wt.% Nafion® ionomer in isopropanol to form a catalyst ink. This ink was then directly sprayed using an automatic spraying system onto one side of a Nafion® 212 polymer membrane. Spraying was controlled to result in a cathode catalyst layer Pt loading of 0.4 mg_{Pt} cm^{-2}. Anodes were prepared using Pt/C in the same fashion with a loading of 0.2 mg_{Pt} cm^{-2} [16]. 250 cm^2 MEAs using commercial Pt/C (Johnson Matthey HiSpec 4000, JM) as anode and cathode catalysts were also prepared for comparison.

2.5. Stack durability testing

In order to evaluate the durability of PtNW/C or commercial Pt/C cathode catalysts, two 1.5 kW stacks composed of 15 individual

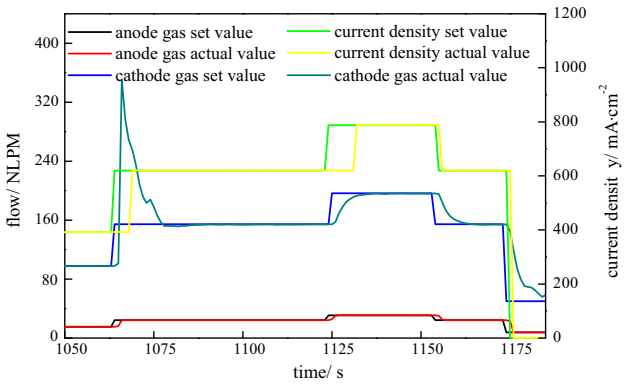

Fig. 5. Gas supplying change for 1.5 kW stack vs. time.

250 cm^2 MEAs were designed. The first stack assembly consisted of a PtNW/C based cathode, and a commercial Pt/C based anode. The second stack assembly consisted of commercial Pt/C at both the cathode and anode. Stack testing was carried out using a G500-30 kW test station (Green light). A dynamic load was applied, derived from actual FC vehicle drum test data which is based on the J1015 driving cycle [17]. The profile of the dynamic load is shown in Fig. 1, whereby the output current density, instead of vehicle speed, is directly displayed. Highlighted in this figure, the load period is 1200 s, the open circuit voltage hold time is 37.9% of the load period, and the peak load during each cycle is 800 mA cm^{-2}. This dynamic load cycling approach was applied in order to simulate the real driving conditions of a FC vehicle, and therefore the results adequately reflect the durability of a FC stack under practical operation. The stack was run at 70 °C, and 60 kPa, with the temperatures of hydrogen and air vapor feeds maintained at 80 °C by tape heaters. Furthermore, a relative humidity (RH) of 100% was maintained using membrane humidifiers [18,19]. Reactant gas flow stoichiometries were fixed at 1.2 and 4 for hydrogen and air, respectively.

3. Results and discussion

In order to investigate the stability of the prepared PtNW/C catalyst materials, half-cell ADT was carried out. A catalyst coated electrode was subjected to 1500 potential cycles from 0.6 to 1.2 V vs RHE at a scan rate of 50 mV s^{-1} under nitrogen saturated conditions. CV curves were obtained initially and immediately following ADT cycling as depicted in Fig. 2A and B for commercial Pt/C and PtNW/C, respectively. PtNW/C was found to provide excellent ECSA retention, maintaining 96.9% of the active surface area after ADT as highlighted in Table 1. This was superior to commercial Pt/C, maintaining only 76.7% of the initial ECSA. This improvement for PtNW/C can be attributed to the one-dimensional nanostructure with lengths in the 20–40 nm range that makes Pt less vulnerable to dissolution, Ostwald ripening, and aggregation during fuel cell operation compared to zero-dimensional Pt nanoparticles [10]. This provides preliminary indication that that the durability of PtNW/C is much better than commercial Pt/C and is consistent with results of previous reports [10–13].

PtNW/C and Pt/C were then fabricated into cathode electrode structures, and a different ADT protocol was carried out using a single cell MEA. Initially, in situ ECSA values were estimated using CV under fully humidified H_2/N_2 conditions. The potential was then held at 1.5 V under fully humidified air/air for 14 h, and after completion, ECSA values were measured again under fully humidified H_2/N_2 [20]. Fig. 3A and B presents CV curves before and after ADT for PtNW/C and commercial Pt/C, respectively. Based

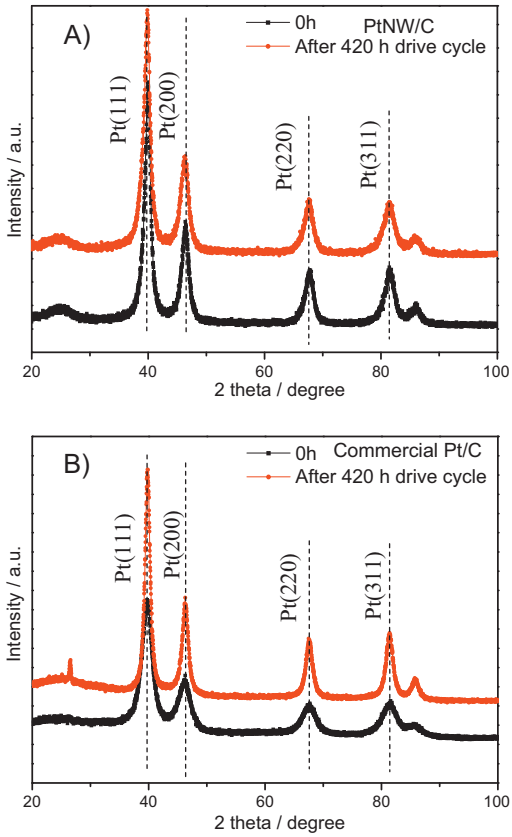

Fig. 6. XRD patterns of (A) PtNW/C cathode before and after 420 h durability testing, and (B) commercial Pt/C cathode before and after 420 h durability testing.

on the charge transfer for hydrogen adsorption/desorption it can be clearly seen that the ECSA of commercial Pt/C after 14 h ADT is significantly reduced, whereas PtNW/C demonstrates only a minor loss. These results further support that the durability of PtNW/C is much better than commercially available Pt/C, particularly when fabricated into practical electrode structures and integrated into a single fuel cell. From these in-situ and ex-situ ADT results, it can be seen that preliminary investigations highlight that as prepared PtNW/C provides improved stability in comparison to Pt/C. Once again this is consistent with the results of previous reports [11–13,21–23], and commonly attributed to the increased stability of extended surface structured Pt in comparison to high surface energy nanoparticles. This indication of the highly promising stability capabilities of PtNW/C inspired us to evaluate its durability as a cathode electrode catalyst under practical operating conditions, particularly a simulated drive cycle in a 1.5 kW fuel cell stack based on this new catalyst technology.

The 1.5 kW stack was composed of 15 individual 250 cm^2 MEA (homemade PtNW/C or commercial Pt/C, as cathode catalyst). The average cell power in the 1.5 kW stack was varied during the 420 h of continuous operation as shown in Fig. 4A and B. From this figure, during the 420 h of testing, the average voltage of every single cell based on PtNW/C cathode electrodes reduced from 0.619 V at 800 mA cm^{-2} to 0.53 V at 800 mA cm^{-2}. During these simulated driving conditions, this represented an average cell decline rate of 14.4%. Conversely, when using commercial Pt/C as both a cathode and anode electrocatalysts, the average decline rate of every single cell after 420 h of dynamic driving cycle durability testing is 17.9% (Fig. 4C and D).

The performance degradation of each stack can be caused by several factors including membrane degradation, ionomer

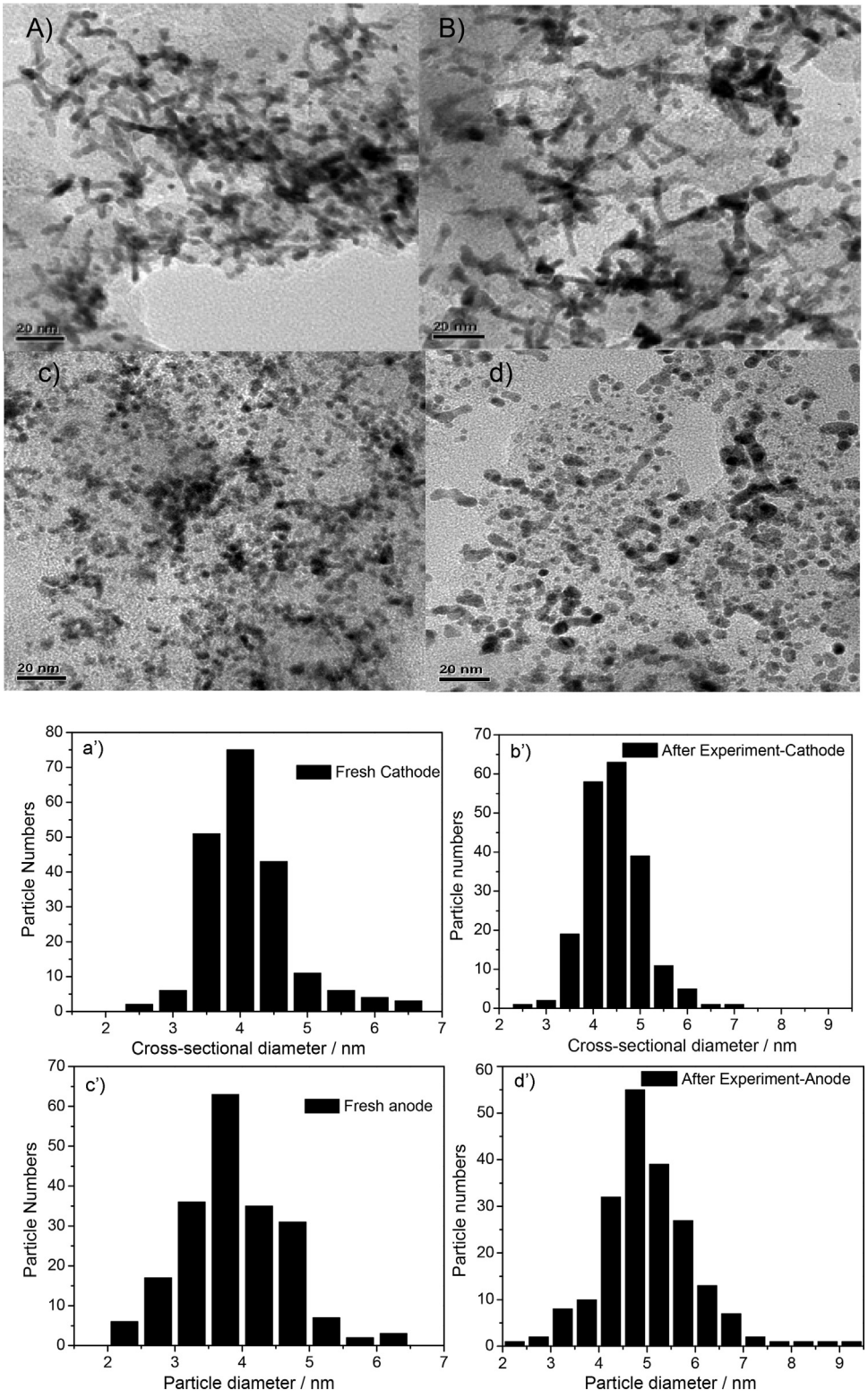

Fig. 7. TEM images and particle size histograms of the cathode PtNW/C before (A), (A′), after (B), (B′) 420 h durability testing, anode commercial Pt/C before (C), (C′) and after (D), (D′) 420 h durability testing.

decomposition, and electrode degradation at both the anode and cathode. The materials, fabrication processes and testing protocols for each stack were however identical, with the exception of either using PtNW/C or Pt/C as the cathode. Therefore keeping all parameters identical, the improved durability of the stack using PtNW/C (14.4% voltage loss) in comparison to the stack using Pt/C (17.9% voltage loss) can be pinpointed directly to the durability of the PtNW/C cathode catalyst. It should also be noted that after each day of testing the stacks were allowed to rest overnight, giving rise to the observed voltage peaks in Fig. 4 that most likely would arise due to beneficial water and thermal management properties arising from the rest that would impact the observed fuel cell voltage [24,25]. With the mechanistic pathways of cell performance degradation investigated and discussed in more detail later on, the improvement in cell performance loss for PtNW/C in comparison to commercial Pt/C can be attributed to the unique catalyst nanostructure of these newly developed materials when integrated into unique cathode architectures and used in a fuel cell stack.

To understand the cause of performance loss in the 1.5 kW fuel cell stacks, Fig. 5 presents the gas supplying changes occurring over time. From this figure, it can be seen that gas supply lagging is observed along with current lagging, which may cause fuel/air starvation within the stack. This phenomenon arises due to the rapid changes in load frequencies, which can lead to anode/cathode catalyst particle growth and aggregation, inevitably affecting the stack durability. On the other hand, from Fig. 1, it can be also seen that OCV time prolongs 37.9% of the drive cycle profile time, which can also cause carbon corrosion, catalyst dissolution and then irreversibly damage the MEAs. It is these harsh conditions encountered during the applied drive cycle that ultimately lead to an accelerated rate of stack degradation.

In order to understand the structural changes of the PtNW/C and commercial Pt/C cathode catalyst after the 420 h drive cycle durability testing, XRD patterns were collected and displayed in Fig. 6 along with the pattern collected for pristine PtNW/C and commercial Pt/C. After testing, negligible changes in peak position, broadening, or height for the (1 1 1), (2 0 0), (2 2 0) and (3 1 1) planes of Pt NW are observable. These results indicate the Pt crystallite structure is very stable throughout the drive cycle testing which exposed the cathode catalyst to potential ranges that encompass the oxidation/reduction potential for Pt that has the propensity to result in higher Pt dissolution rates than just holding potential in the oxidation region [26,27]. However, changes in the intensity of the peaks for the (1 1 1), (2 2 0) and (3 1 1) planes of Pt particles are observed after 420 h of drive cycle durability testing. Therefore it can be concluded that commercial Pt/C catalyst is not stable throughout the drive cycle testing.

In addition, the TEM images and particle size histograms of PtNW/C before and after the 420 h drive cycle durability testing are displayed in Fig. 7A, A′, B and B′, respectively. These figures depict the PtNW uniformly distributed on carbon with an average cross-sectional diameter of 4.0 ± 0.2 nm and length of 20–40 nm, along with minimal changes observed after the durability testing.

CV curves for the PtNW/C cathode were obtained prior to and immediately following the 420 h of durability testing and are displayed in Fig. 8. PtNW/C demonstrated exemplary ECSA retention, maintaining 99% of their original ECSA. ORR polarization curves before and after 420 h of durability testing are also provided in Fig. 9. PtNW/C displayed high ORR activity and exemplary activity, where almost identical polarization curves were observed before and after the 420 h of durability testing.

With minimal structural, ECSA and ORR activity changes observed at the PtNW/C based cathode, the commercial Pt/C used at the anode of this fuel cell stack was also imaged by TEM in an attempt to pinpoint the source of performance loss after 420 h of drive cycle testing. TEM images and particle size histograms of the anode Pt/C materials are provided before and after testing in Fig. 7C, C′, D and D′, respectively. Clearly, significant Pt nanoparticle growth and aggregation is observed after drive cycle testing, most likely arising due to the harsh fuel/air starvation conditions that were induced by the particular testing regime utilized. Based on these characterizations, it is apparent that the fuel cell stack performance loss resulted from the degradation of the commercial Pt/C catalyst utilized at the anode.

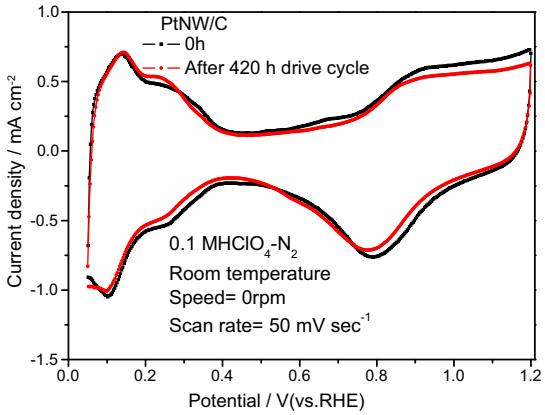

Fig. 8. Cyclic voltammograms for O_2 on PtNW/C before (A) and after (B) 420 h durability testing in 0.1 M $HClO_4$ at the ambient solution temperature in O_2; scan rate: 50 mV s^{-1}, electrode area: 0.283 cm^2; catalyst loading: 28 μg cm^{-2}.

The second fuel cell stack, using commercial Pt/C as both the cathode and electrode catalyst was also characterized before and after 420 h of drive cycle testing. TEM images and particle size histograms of the anode and cathode Pt/C materials are provided before and after testing in Fig. 10A, A′, B, B′, C, C′, D and D′, respectively. From this figure, it can be seen that the commercial Pt/C anode catalyst underwent particle growth in a fashion similar to the first fuel cell stack. Furthermore, the cathode Pt/C catalyst also demonstrated severe Pt nanoparticle growth and aggregation. Therefore, it can be concluded that the inferior durability of the second fuel cell stack results from the lower stability of commercial Pt/C when utilized as cathode electrode materials in comparison to as prepared PtNW/C.

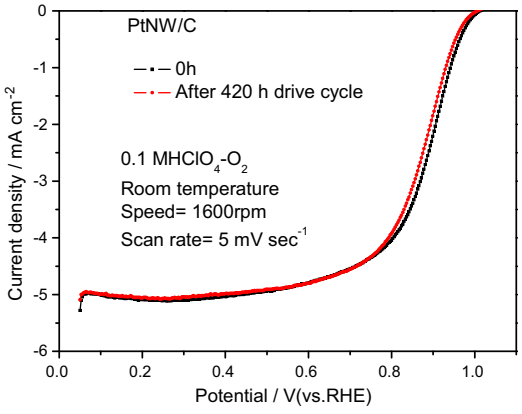

Fig. 9. Linear scan voltammograms for O_2 on PtNW/C before (A) and after (B) 420 h durability testing in 0.1 M $HClO_4$ at the ambient solution temperature in O_2; Rotation speed: 1600 rpm, scan rate: 5 mV s^{-1}, electrode area: 0.283 cm^2; catalyst loading: 28 μg cm^{-2}.

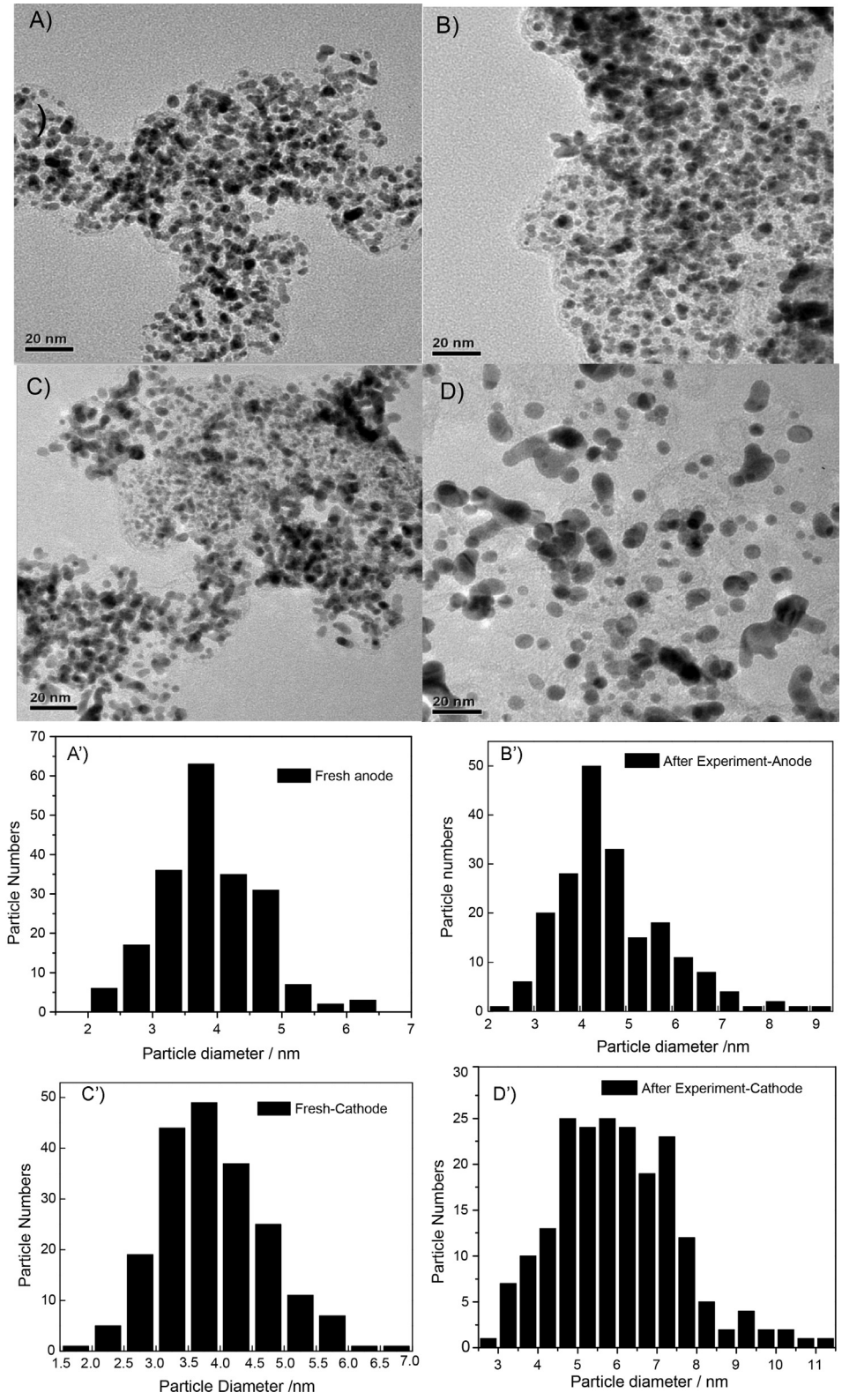

Fig. 10. TEM images and particle size histograms of the anode commercial Pt/C before (A), (A′), after (B), (B′) 420 h durability testing, cathode commercial Pt/C before (C), (C′) and after (D), (D′) 420 h durability testing.

4. Conclusions

In summary, PtNW/C materials were synthesized by a simple and inexpensive template-free methodology. Preliminary in-situ and ex-situ ADT protocols indicated superior stability of the PtNW/C in comparison to commercial Pt/C, attributed to its increased resilience to Pt dissolution, Ostwald ripening and agglomeration. Owing to these promising results, for the first time PtNW/C were assembled into a fuel cell stack and tested for performance and stability under practical conditions. A 1.5 kW PEMFC

stack consisting of 15 individual cells with an active area of 250 cm^2 was employed. After 420 h of a simulated drive cycle in which the stack was exposed to harsh operative conditions including fuel/air starvation arising from rapidly changing load frequencies, the average voltage of each individual cell based on PtNW/C cathode and a commercial Pt/C anode reduced from 0.619 V at 800 mA cm^{-2} to 0.53 V at 800 mA cm^{-2}, representing an average decline rate of 14.4%. It was found that this performance loss occurred due to degradation of the Pt/C based anode catalysts in the form of Pt nanoparticle growth and aggregation, whereby the structure, ECSA and ORR activity of the PtNW/C cathode remained relatively unchanged. Conversely, when using commercial Pt/C as both an anode and cathode catalyst, higher (17.9%) performance loss was observed, along with clear degradation of the Pt/C cathode catalyst materials observed based on post treatment characterization. Therefore, the 1.5 kW PEMFC stack employing PtNW/C as the cathode structures was found to provide enhanced stability under practical drive cycle conditions in comparison to commercial Pt/C. From these results, PtNW/C materials can be considered promising replacements to conventional Pt/C nanoparticle catalysts as cathode materials for PEMFCs applications.

Acknowledgments

The authors appreciate the National Natural Science Foundation of China (No. 21206128), International Postdoctoral Exchange Fellowship Program of China (201372) and MOST (2012AA110501, 2013BAG15B00) for the financial support of this work. Also, this work was partly financed by Henkel Professorship of Tongji University.

References

[1] B. Li, D.C. Higgins, S.M. Zhu, H. Li, H.J. Wang, J.X. Ma, Z.W. Chen, Catal. Commun. 18 (2012) 51.
[2] G. Escobedo, M. Gummalla, R.B. Moore, FY 2006 Annual Progress Report, 2006, pp. 706.
[3] B. Hwang, S. Kuma, C. Chen, M. Monalisa, D. Cheng, J. Liu, J. Phys. Chem. C 111 (2007) 15267.
[4] R. Narayanan, M. El-Sayed, Langmuir 21 (2005) 2027.
[5] Z.W. Chen, M. Waje, W. Li, Y.S. Yan, Angew. Chem. Int. Ed. 46 (2007) 4060.
[6] D.C. Higgins, S. Ye, S. Knights, Z.W. Chen, Electrochem. Solid-State Lett. 15 (2012) B83.
[7] B. Li, Z.Y. Yan, D.C. Higgins, D.J. Yang, Z.W. Chen, J.X. Ma, J. Power Sources 262 (2014) 488.
[8] S.G. Wang, S.P. Jiang, X. Wang, J. Guo, Electrochim. Acta 56 (2011) 1563.
[9] C.C. Chien, K.T. Jeng, Mater. Chem. Phys. 103 (2007) 400.
[10] S.H. Sun, G.X. Zhang, D.S. Geng, Y.G. Chen, R.Y. Li, M. Cai, X.L. Sun, Angew. Chem. Int. Ed. 50 (2011) 422.
[11] S.H. Sun, F. Jaouen, J.P. Dodelet, Adv. Mater. 20 (2008) 3900.
[12] S.H. Sun, D.Q. Yang, D. Villers, G.X. Zhang, E. Sacher, J.P. Dodelet, Adv. Mater. 20 (2008) 571.
[13] S.H. Sun, D.Q. Yang, G.X. Zhang, E. Sacher, J.P. Dodelet, Chem. Mater. 19 (2007) 6376.
[14] B. Li, D.C. Higgins, D.J. Yang, H. Lv, Z.P. Yu, J.X. Ma, Int. J. Hydrogen Energy 38 (2013) 5813.
[15] B. Li, D.C. Higgins, D.J. Yang, H. Lv, Z.P. Yu, J.X. Ma, Int. J. Hydrogen Energy 37 (2012) 18843.
[16] B. Li, J.L. Qiao, D.J. Yang, R. Lin, H. Lv, H.J. Wang, J.X. Ma, Int. J. Hydrogen Energy 35 (2010) 5528.
[17] B. Li, R. Lin, D.J. Yang, J.X. Ma, Int. J. Hydrogen Energy 35 (2010) 2814.
[18] B. Li, J.L. Qiao, D.J. Yang, J.S. Zheng, J.X. Ma, J.J. Zhang, H.J. Wang, Electrochim. Acta 54 (2009) 5614.
[19] D.J. Yang, J.X. Ma, L. Xu, M.Z. Wu, H.J. Wang, Electrochim. Acta 51 (2006) 4039.
[20] B. Podlovechenko, G. Shterev, R. Semkova, E. Kolyadko, J. Electroanal. Chem. 224 (1987) 225.
[21] R. Wang, D.C. Higgins, M.A. Hoque, D.U. Lee, F. Hassan, Z.W. Chen, Sci. Rep. 3 (2013) 2431.
[22] D.C. Higgins, J. Choi, J. Wu, A. Lopez, Z.W. Chen, J. Mater. Chem. 21 (2012) 3727.
[23] D.C. Higgins, D. Meza, Z.W. Chen, J. Phys. Chem. C 114 (2010) 21982.
[24] R.C. Jiang, H.R. Kunz, J.M. Fenton, J. Power Sources 150 (2005) 120.
[25] M.M. Saleh, T. Okajima, M. Hayase, F. Kitamura, T. Ohsaka, J. Power Sources 164 (2007) 503.
[26] X.P. Wang, R. Kumar, D.J. Myers, Electrochem. Solid-State Lett. 9 (2006) A225.
[27] D.J. Yang, B. Li, H. Zhang, J.S. Zheng, R. Lin, J.X. Ma, J. Power Sources 199 (2012) 68.